A Very Wide-Band Microwave MESFET Mixer Using the Distributed Mixing Principle

ON SAN A. TANG AND COLIN S. AITCHISON

Abstract—A new theory of distributed (traveling-wave) mixing is presented. A closed-form expression for the conversion gain is derived. Subsequently, the expression is reduced to a very simple form when the mixer approaches the ideal lossless case. A simplified nonlinear model of a GaAs MESFET is also described.

Design criteria and considerations are presented. The relative contributions made by circuit parasitics to the conversion gain–bandwidth product are also examined.

Experimental verification on a two-section design is described. It exhibits around 4 dB of conversion loss over the signal frequency band from 2 GHz to the cutoff at 10 GHz for an IF of 1.5 GHz. Experimental results obtained corroborate the theoretical predictions. Better performance is expected if more sections are employed.

I. Introduction

THE USE OF FET'S instead of diodes as low-noise mixers at UHF is a frequent practice. Their successful application in the microwave frequency region has been made possible with the advent of microwave GaAs MESFET's.

The first microwave MESFET mixer was reported by Sitch and Robson [1] in 1973. The MESFET mixer then immediately gained widespread attention in the microwave field because of its distinctive attributes, which include conversion gain instead of the usual conversion loss associated with conventional diode mixers, low-noise figure, and high dynamic range. In 1976, Pucel, Masse, and Bera [2] developed detailed analytical theories to model the performance of a MESFET mixer, which has since been extensively investigated. Recently, Tie and Aitchison [4] presented a detailed theoretical analysis of its noise behavior and that of the effects of parasitic terminations on conversion gain.

Recent years have seen a strong demand for multi-octave microwave components in satellite communication systems and modern radars. Very wide-band microwave diode mixers have been available for many years, but so far, only narrow-band MESFET resonant mixers have been reported. In pursuit of a microwave wide-band MESFET mixer, an original and novel concept of distributed (or traveling-wave) mixing has been proposed and developed by the authors [6]. It is essentially based on the principle of distributed amplification first proposed in 1937 by Percival [7]. With the advent of microwave GaAs MESFET's, interest in the area of distributed amplification has increased considerably in recent years [8]–[11].

In this paper, the theory of distributed mixing using hybrid technology is presented. To confirm the theory, a simple two-section design was constructed and characterized. Agreement with theory is good.

II. Theory

Consider a unilateral simplified model of a distributed mixer incorporating an input gate line and an output drain line, as shown in Fig. 1. The output capacitance C_{ds} and input capacitance C_{gs} of each MESFET are combined with external lumped inductors (L_1 and L_2) and padding capacitances (C_{pad}) to form two lumped-element artificial transmission lines. The gate and drain capacitances form the shunt elements of the two artificial transmission lines.

In the interest of avoiding complicated initial analysis, we will adopt the simple unilateral model of a MESFET depicted in Fig. 2. The two artificial transmission lines are, therefore, coupled only through the MESFET's transconductances, and additional propagation modes due to the presence of MESFET feedback elements (C_{dg} and R_s, for example) have been ignored. g_m, R_{ds}, and C_{gs} are assumed to be the only nonlinear elements [2]–[5] in a MESFET equivalent circuit that yield mixing under the modulation effect of the large-signal local oscillator (LO), and g_m is assumed [2]–[5] to be the predominant nonlinearity in the case of a gate mixer configuration considered here. C_{gs} and R_{ds} will, therefore, be replaced by their time average values [2]–[5].

The RF and LO signals are injected into the gate line through a directional coupler at the left-hand end of the gate line, as is illustrated schematically in Fig. 1. To lower the LO drive requirement, the coupler can be eliminated if the three other possible distributed mixer configurations are employed, namely, the distributed source mixer, where the LO is injected into an additional artificial transmission line (the source line), the distributed dual-gate mixer, where

Manuscript received March 14, 1985; revised July 8, 1985. This work was supported in part by Marconi Defence Systems, Ltd., Stanmore, England.

O. S. A. Tang is with the Department of Electronics, Chelsea College, now called King's College (KQC), University of London, Pulton Place, London SW6 5PR, England.

C. S. Aitchison was with the Department of Electronics, Chelsea College, now called King's College (KQC), University of London. He is now with ERA Technology, Ltd., Cleeve Rd., Leatherhead, Surrey, KT22 75A, England.

0018-9480/85/1200-1470$01.00 ©1985 IEEE

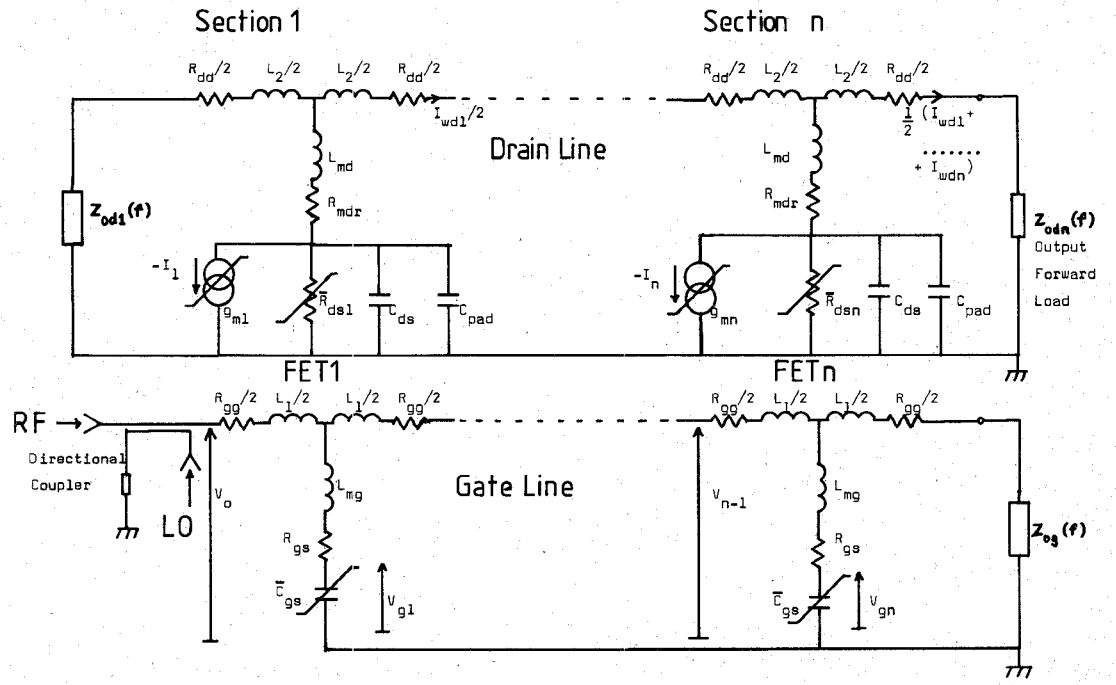

Fig. 1. Schematic of the unilateral model of a traveling-wave mixer employing n MESFET's.

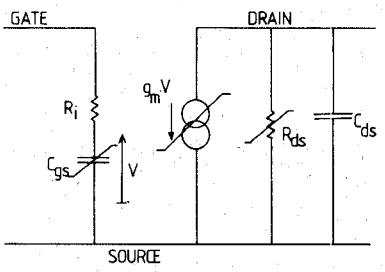

Fig. 2. A unilateral large-signal model of a microwave GaAs MESFET comprised of three nonlinear elements: C_{gs}, g_m, and R_{ds}.

the LO is injected into a second gate line, and finally the distributed drain mixer, where the LO is injected into the idle port of the drain line.

The analysis of the mixer circuit consists of two parts; the nonlinear analysis dealing with the injection of a single-tone LO large signal and the linear analysis dealing with the small-signal mixing products.

A. Nonlinear Analysis

We will assume a quasi-static system, whereby all the circuit components and device characteristics are time invariant and frequency independent. We will also assume that the LO signal is a sine wave. The frequency harmonics of $g_m(t)$, $R_{ds}(t)$, and $C_{gs}(t)$ can be obtained by utilizing the Fourier series. For example, the time-varying transconductance can be represented as

$$g_m(t) = \sum_{p=-\infty}^{\infty} b_p \cdot e^{jp\omega_{LO}t}$$

$$b_p = \frac{1}{T_{LO}} \int_{-T_{LO}/2}^{T_{LO}/2} g_m(t) \cdot e^{-jp\omega_{LO}t}\, dt. \qquad (1)$$

Both the discrete Fourier transform [12] and the fast Fourier transform [12] can be subsequently used to evaluate the contents of the above expression. In the case of $R_{ds}(t)$ and $C_{gs}(t)$, only the dc components are required. Assuming that the harmonics of $g_m(t)$ for a given LO drive level and dc bias condition have been obtained, $g_m(t)$ can now be represented as

$$g_m(t) = \bar{g}_m + \sum_{p=1}^{\infty} \left[g'_p \cdot e^{jp\omega_{LO}t} + g'_{-p} \cdot e^{-jp\omega_{LO}t} \right] \qquad (2)$$

where g'_p and g'_{-p} are complex Fourier coefficients. However, because $g_m(t)$ is a purely real-time function, we have

$$g'_p = (g'_{-p})^*$$

where the asterisk * denotes the complex conjugate.

As there can be several MESFET's in a distributed mixer, we denote the time-varying transconductance of the first FET as $g_{m1}(t)$. Its Fourier transform $G_{m1}(f)$ is given by

$$\bar{g}_{m1} \cdot \delta(f) + g'_{11} \cdot \delta(f - f_{LO}) + g'_{-11} \cdot \delta(f + f_{LO}) + g'_{21} \cdot \delta(f - 2f_{LO}) + g'_{-21} \cdot \delta(f + 2f_{LO}) + \cdots \qquad (3)$$

where $\delta(f)$ is the standard delta impulse frequency function.

Consider that $g_{m1}(t)$, $g_{m2}(t)$, $g_{m3}(t), \cdots, g_{mn}(t)$ are calculated on the assumption that the LO signals at each of the gates of the FET's are all in phase, so in order to take into account the relative phase shift of the LO signals between FET's in the gate line, we can denote the Fourier

transform of the transconductance as

$$G_{m1}(f)\cdot e^{j\phi_{\text{arb}}(f)} \qquad \text{for the first FET}$$

$$\vdots$$

and

$$G_{mn}(f)\cdot e^{-j[(n-1)\cdot\beta_g(f)-\phi_{\text{arb}}(f)]} \qquad \text{for the } n\text{th FET}$$

where $\beta_g(f)$ is the phase shift per gate section and $\phi_{\text{arb}}(f)$ is an arbitrary phase difference between the LO and RF signals at the gate of the first FET.

B. Linear Analysis

If we assume that the RF signal is much smaller than that of the LO signal, the small-signal mixing products generated by the input RF signal can be considered as linear [2]–[5]. The primary source of IF comes from the interaction between the RF input signal and the conversion transconductance (g_1). There are many other secondary sources of IF, including the interaction between the image component generated in the drain line and fed back into the gate line with g_1, the interaction between the sum component and g_2, among many others. However, because of the unilateral assumption made earlier, these secondary sources are ignored.

The key to the design of a distributed mixer is to allow the LO and RF signals to propagate down the gate line with the minimum attenuation, as well as to ensure that all the IF output currents generated at the drain of each FET propagate and arrive at the forward drain output termination in phase.

In essence, the concept of distributed mixing is based on the idea of separating the input as well as output capacitances of the MESFET's connected in parallel by means of artificial transmission lines, while effectively adding their conversion transconductances.

Fig. 1 shows the first and the nth section of the gate line, where L_{mg} is the effective bond wire inductance of the gate and source, R_{gs} is the sum of the internal FET gate loss R_i and that of the source grounding path, and R_{gg} is the resistive loss of the inductor L_1. By means of two-port transmission matrices, the characteristic impedance $Z_{0g}(f)$, the propagation function per section $\gamma_g(f)$, which is equal to $\alpha_g(f)$ plus $j\cdot\beta_g(f)$, as well as $\Delta(f)$, where $V_{gn}=\Delta(f)\cdot V_{n-1}$, can be expressed as functions of the circuit elements.

Contrary to the case of the parameters in a lossy gate line section mentioned above, which are assumed to be identical for every section due to the fact that $\bar{C}_{gs}$ is the same for every section (because of the approximate linear dependence of C_{gs} on the gate bias in the current saturation region), the parameters in a lossy drain line differ from one section to another because R_{ds} is a function of LO signal which is altered both in magnitude and phase as it propagates down the gate line towards the idle load. Hence, for an nth drain line section, the characteristic impedance $Z_{0dn}(f)$, the propagation function $\gamma_{dn}(f)$, which is equal to $\alpha_{dn}(f)$ plus $j\cdot\beta_{dn}(f)$, can be expressed as functions of the circuit elements of the nth section.

A single-sideband representation of voltages and currents is adopted in the following analysis. V_0 and V_{g1} are RF voltages defined in Fig. 1 and are related by the following expression:

$$V_{g1}=\Delta(f_{\text{RF}})\cdot V_0. \tag{4}$$

It can be shown that

$$V_{gn}=\Delta(f_{\text{RF}})\cdot V_0\cdot e^{-(n-1)\cdot(\alpha_g(f_{\text{RF}})+j\beta_g(f_{\text{RF}}))}. \tag{5}$$

In addition, it can also be proved that the current generator output of the nth FET is given by

$$\begin{aligned}&\{\hat{V}_0\cdot\delta(f+f_{\text{RF}})\cdot\Delta^*(f_{\text{RF}})\\&\quad\cdot e^{-(n-1)\cdot(\alpha_g(f_{\text{RF}})+j\beta_g(f_{\text{RF}}))^*}\}\\&\circledast\{G_{mn}(f)\cdot e^{-j((n-1)\cdot\beta_g(f)-\phi_{\text{arb}}(f))}\}\end{aligned} \tag{6}$$

such that

$$G_{mn}(f)=\bar{g}_{mn}\cdot\delta(f)+\sum_{p=-\infty}^{\infty}g'_{pn}\cdot\delta(f-pf_{\text{LO}}) \tag{7}$$

and $\circledast$ denotes a frequency convolution process [12].

After expansion and algebraic manipulation, the IF component of the nth current generator is given by

$$\begin{aligned}&\{\hat{V}_0\cdot\Delta^*(f_{\text{RF}})\cdot g'_{1n}\cdot e^{-(n-1)\cdot\alpha_g(f_{\text{RF}})}\}\\&\quad\cdot\{e^{j[(n-1)\cdot\beta_g(f_{\text{RF}})-(n-1)\cdot\beta_g(f_{\text{LO}})+\phi_{\text{arb}}(f_{\text{LO}})]}\}\\&\quad\cdot\{\delta(f-f_{\text{IF}})\}.\end{aligned} \tag{8}$$

The total vector sum of all the IF currents propagating from each section to the forward drain line load can be calculated. Supposing that this is denoted by I_{IF}; then the mean output IF power is given by

$$P_{\text{IF}}=\frac{|I_{\text{IF}}|^2}{2}\cdot\text{Re}(Z_{dT}(f_{\text{IF}})). \tag{9}$$

The available input RF power with 50-Ω terminations can be proved to be

$$P_{\text{RF}}=\frac{\hat{V}_0^2}{400}\cdot|A+B/Z_{\text{in}}(f_{\text{RF}})|^2\,|1+50/Z'_{\text{in}}(f_{\text{RF}})|^2 \tag{10}$$

where $Z_{dT}(f)$, $Z_{\text{in}}(f)$, and $Z'_{\text{in}}(f)$ are input impedances defined in Fig. 3, and

$$\begin{bmatrix}A & B\\ C & D\end{bmatrix}$$

is the transmission matrix of the gate line matching network.

The RF to IF conversion transducer gain is given by $10\cdot\text{Log}_{10}(P_{\text{IF}}/P_{\text{RF}})$ in decibels.

Having established this general formulation for the hybrid design, we will consider the ideal limiting case of a perfectly matched ideal lossless mixer, whereby R_{gg}, L_{mg}, R_{gs}, R_{dd}, L_{md}, and R_{mdr} are all zero, while R_{ds} is infinitely large. The LO, RF, and IF signals are only altered in phase as they propagate down the gate and drain lines, respectively.

With appropriate substitutions and simplifications, it can be shown that the conversion gain expression, $P_{\text{IF}}/P_{\text{RF}}$,

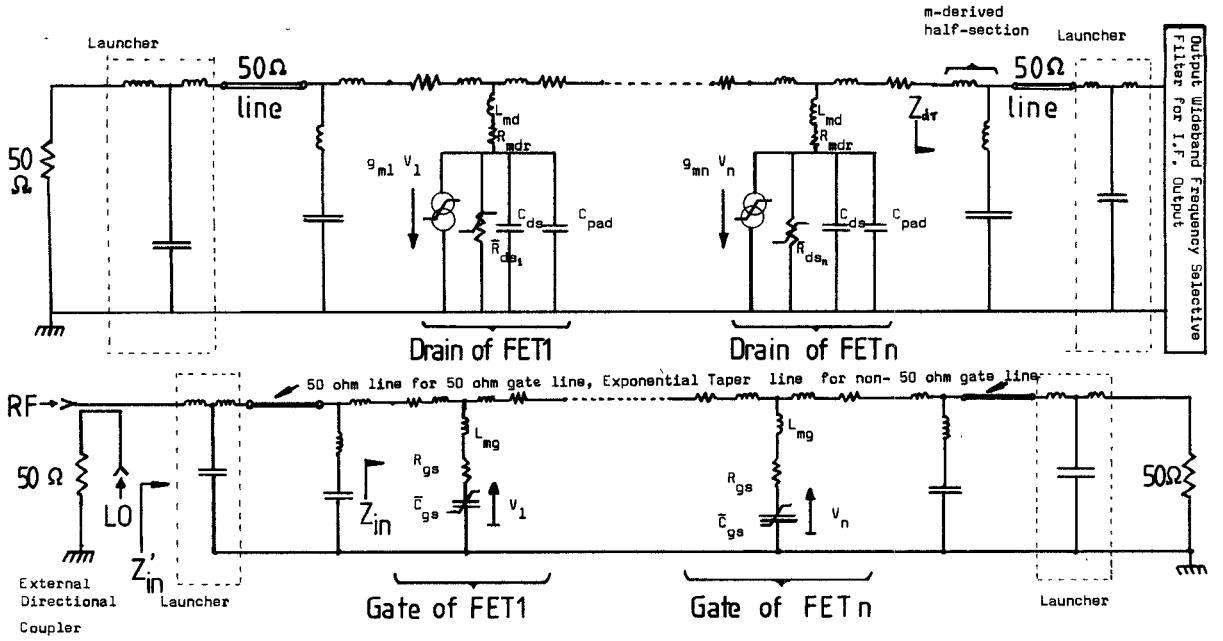

Fig. 3. Equivalent circuit of a traveling-wave mixer realized in discrete hybrid form and comprised of a 50-Ω input gate line and a 50-Ω output drain line (dc biasing circuits are not shown).

can be reduced to the simple form as shown below in this ideal lossless limiting case

$$\frac{g_1^2}{16}\cdot Z_{d\pi}(f_{\mathrm{IF}})\cdot Z_{g\pi}(f_{\mathrm{RF}})\cdot\left|\frac{\sin(n\theta/2)}{\sin(\theta/2)}\right|^2 \tag{11}$$

where $g_1 = 2|g_1'| = 2|g'_{-1}|$, $Z_{d\pi}(f)$ and $Z_{g\pi}(f)$ are the π section characteristic impedances of the drain and gate lines, respectively, and θ is equal to

$$\beta_g(f_{\mathrm{LO}}) - \beta_g(f_{\mathrm{RF}}) - \beta_d(f_{\mathrm{IF}}). \tag{12}$$

$$\theta = 0 \tag{13}$$

Equation (13) has to be satisfied in order to maximize the conversion gain and then (11) simplifies to the following expression at one value of f_{RF}, for a given set of values of f_{IF} and the cutoff frequencies of the gate and drain lines:

$$\frac{n^2 g_1^2 Z_{d\pi}(f_{\mathrm{IF}}) Z_{g\pi}(f_{\mathrm{RF}})}{16}. \tag{14}$$

The gain of an ideal lossless unilateral n-section distributed amplifier valid up to the cutoff frequency when $\beta_g(f)$ is made equal to $\beta_d(f)$ is given by [11]

$$\frac{n^2 g_m^2 Z_{d\pi}(f) Z_{g\pi}(f)}{4} \tag{15}$$

and it can be seen that the two expressions (14) and (15) are of the same mathematical form. The factor of 4 difference between the two expressions arises due to the fact that a mixer utilizes the trigonometric identity that expands the product of the two cosine terms into sum and difference frequencies

$$\cos(A)\cdot\cos(B) = \tfrac{1}{2}(\cos(A-B)+\cos(A+B)). \tag{16}$$

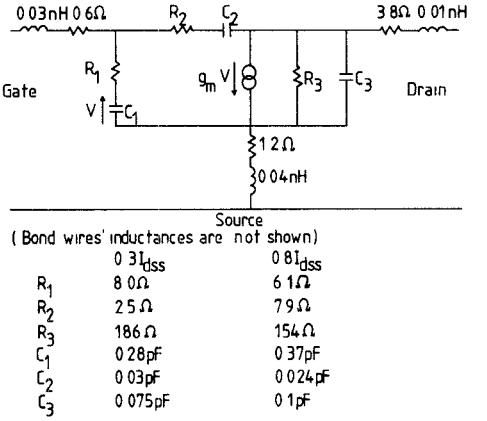

	0 3I_{dss}	0 8I_{dss}
R_1	8 0Ω	6 1Ω
R_2	2 5Ω	7 9Ω
R_3	186Ω	154Ω
C_1	0 28pF	0 37pF
C_2	0 03pF	0 024pF
C_3	0 075pF	0 1pF

Fig. 4. The 2–18-GHz small-signal computer-optimized equivalent circuit of the NEC NE71000 chip. (NB. Transconductance and transit time for $0.3I_{dss}$ bias are 50 mmho and 1.6 pS, respectively, and 73 mmho and 2.2 pS, respectively, for $0.8I_{dss}$ bias.)

A computer program has been written, which will compute the conversion gain of a traveling-wave mixer implemented in hybrid form, provided that the appropriate Fourier components of g_m, R_{ds}, and C_{gs} under a stated dc bias and LO drive level have been evaluated from the separate nonlinear analysis of the circuit. This will serve as a useful CAD tool for mixer design and characterization.

III. MESFET Modeling

A simplified unilateral nonlinear model of the NEC NE71000 GaAs MESFET chip under LO excitation has been developed. It is based on small-signal 2–18-GHz s-parameter microwave measurements at two different bias points ($0.3I_{dss}$ and $0.8I_{dss}$) in the current saturation region ($V_{DS} = 3$ V), as well as dc and low-frequency (2 MHz) characterization.

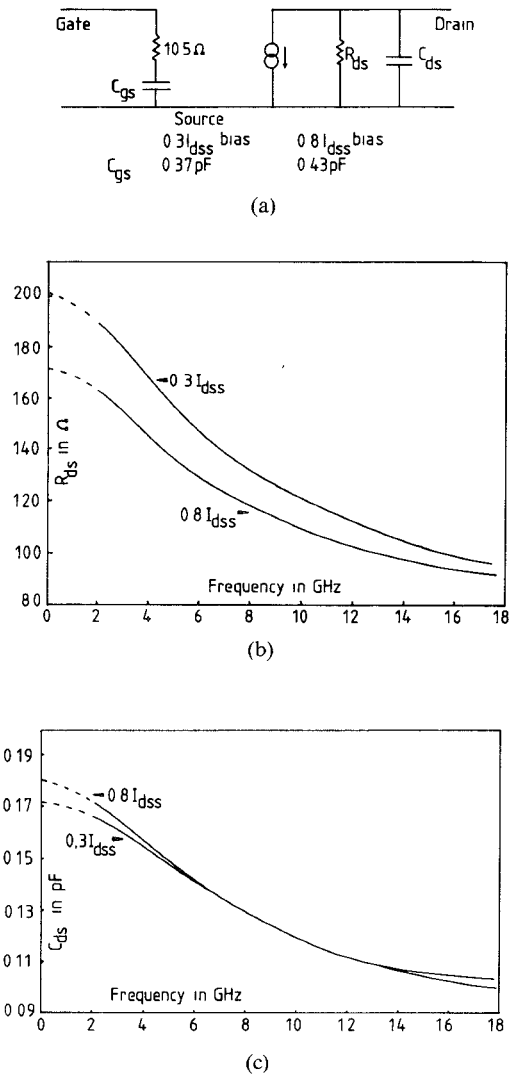

Fig. 5. (a) The 2–18-GHz small-signal computer-optimized unilateral equivalent circuit of the NEC NE71000 chip (the values of R_{ds} and C_{ds} are shown in Fig 5(b) and (c), respectively). (b) Variation of R_{ds} in the optimized unilateral circuit of Fig. 5(a) with frequency. (c) Variation of C_{ds} in the optimized unilateral circuit of Fig. 5(a) with frequency.

The computer-optimized (employing the quasi-Newton minimization algorithm) small-signal linear equivalent circuit at $0.3I_{dss}$ and $0.8I_{dss}$ is shown in Fig. 4. In this connection, it may be of interest to point out that, as the name implies, an equivalent circuit may not have any real physical significance, and it merely represents a nodal connection of electrical elements which just happen to provide the best curve fit of the measured results.

Based on these results, the optimized unilateral equivalent circuit at $0.3I_{dss}$ and $0.8I_{dss}$, assuming 50-Ω terminations at the gate and drain, is shown in Fig. 5(a)–(c). The striking dependence of both R_{ds} and C_{ds} on frequency explains why a single unilateral model is an unrealistic representation of the drain of the MESFET over any other than a narrow band of frequency. However, since the IF band usually occupies the low-frequency end of the passband in the drain line and has a relatively narrow bandwidth, a unilateral model in that frequency range is considered as sufficiently accurate for our purposes here.

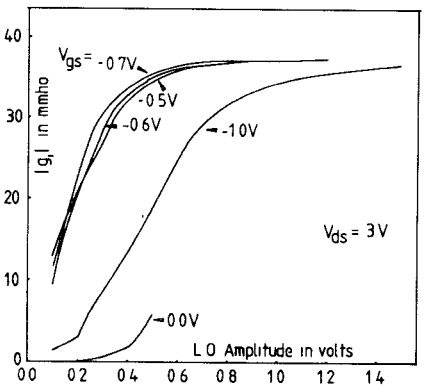

Fig. 6. The magnitudes of conversion transconductance versus LO amplitude with dc gate bias as a parameter.

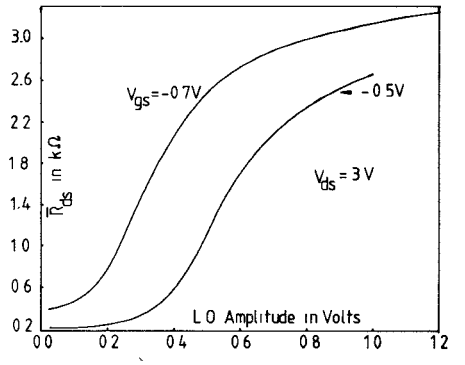

Fig. 7. Variation of the time-average (or dc component of the Fourier series) output resistance R_{ds} with LO amplitude, with dc gate bias as a parameter.

The bias dependence of g_m was obtained from dc I–V curves [4]. The variation of the magnitudes of the first Fourier harmonic of $g_m(t)$ with LO amplitude is shown in Fig. 6. Since the g_1 characteristic flattens out when the LO voltage amplitude across C_{gs} exceeds +0.6 V (for gate bias between −0.5 and −0.7 V), higher LO drive level contributes very little additional transconductance nonlinearity.

The bias dependence of R_{ds} was obtained from measurements based on the substitution technique at 2 MHz, taking into account the frequency dispersion behavior of R_{ds} [13]. The results are close to values extrapolated from microwave values shown in Fig. 5(b) at the same bias points. The variation of the dc component of $R_{ds}(t)$ with LO amplitude is depicted in Fig. 7.

Measurements show that g_m, R_{ds}, and C_{gs} are predominantly gate bias dependent, and approximately independent of drain bias when biased in the current saturation region.

IV. Design Criteria and Considerations

The effects of internal MESFET losses as well as circuit parasitics associated with thin-film hybrid design on conversion gain have been extensively investigated, both theoretically and practically.

Figs. 8–10 show the variation of attenuation per gate section with normalized frequency when R_{gs}, L_{mg}, and R_{gg}, respectively, increase above their zero ideal values. It

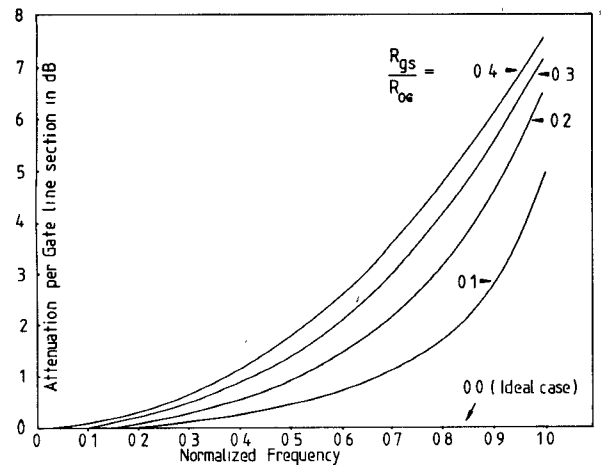

Fig. 8. Attenuation per gate line section versus normalized frequency, with R_{gs}/R_{OG} as a parameter (dc characteristic impedance $R_{OG} = 50$ Ω, cutoff frequency (ideal) = 22.7 GHz, $L_{mg} = 0$, $R_{gg} = 0$).

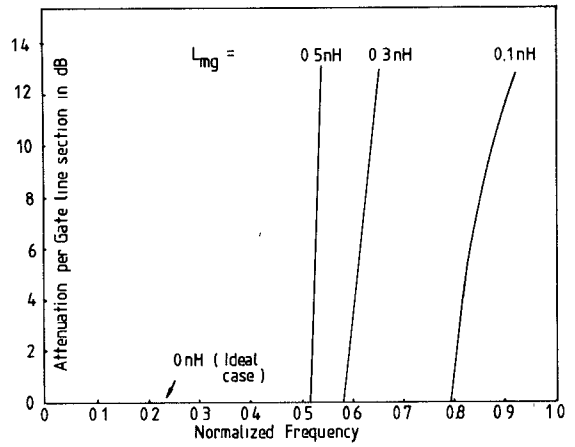

Fig. 9. Variation of attenuation per gate line section with normalized frequency, with L_{mg} as a parameter (dc Characteristic impedance $R_{OG} = 50$ Ω, cutoff frequency (ideal) = 22.7 GHz, $R_{gs} = 0$, $R_{gg} = 0$).

implies that gate resistive loading R_{gs} is mainly responsible for the conversion gain rolloff and reduction in signal bandwidth, while gate inductive loading L_{mg} is the predominant factor in bandwidth curtailment.

Fig. 11 examines the variation of attenuation per drain section with normalized frequency when the drain resistive shunt loading $\bar{R}_{ds}$ decreases from the ideal value of infinity. For low values of $\bar{R}_{ds}$, there is a selective attenuation of high frequencies. However, the MESFET is normally biased near pinchoff and $\bar{R}_{ds}$ tends to be several times bigger than R_{OD}, and attenuation occurs nearly uniformly over the whole passband. For $\bar{R}_{ds}$ greater than $10R_{OD}$, the rate of improvement of attenuation with increasing $\bar{R}_{ds}$ decreases several fold. Because the IF range lies in the low-frequency end of the passband of the drain line, the ill effects of L_{md}, R_{mdr}, and R_{dd} on conversion gain are generally negligible.

It is worthwhile commenting that the aforementioned high-frequency rolloff effect due to gate resistive loading is in fact counteracted somewhat by the rising characteristic of the midshunt π section characteristic impedance actu-

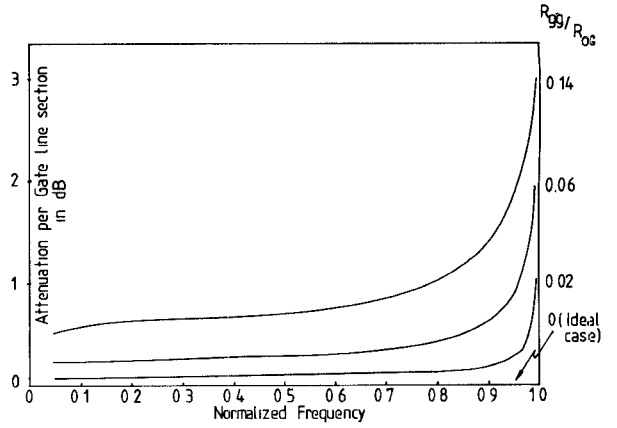

Fig. 10. Variation of attenuation per gate line section with normalized frequency, with R_{gg}/R_{OG} as a parameter (dc characteristic impedance $R_{OG} = 50$ Ω, cutoff frequency (ideal) = 22.7 GHz, $R_{gs} = 0$, $L_{mg} = 0$).

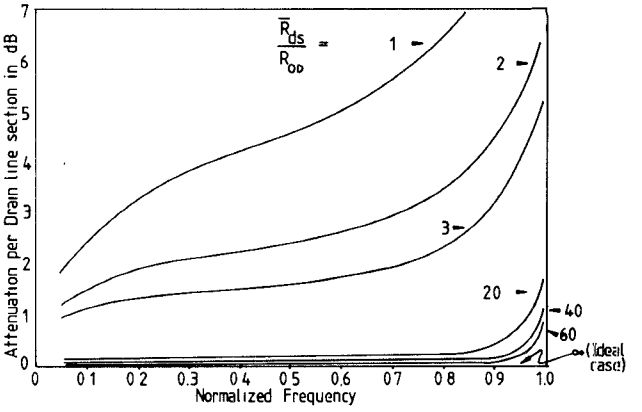

Fig. 11. Variation of attenuation per drain line section with normalized frequency, with R_{ds}/R_{OD} as a parameter (dc characteristic impedance $R_{OD} = 50$ Ω cutoff frequency (ideal) = 22.7 GHz, $R_{mdr} = 0$, $L_{md} = 0$, $R_{dd} = 0$).

ally seen by each MESFET, which causes voltage peaking towards the cutoff frequency. The fact that both the conversion transconductance g_1 and $\bar{R}_{ds}$ of each section depend on LO voltage across its C_{gs} means that the gradual attenuation of voltage in successive section in the gate line will reduce both the input RF signal as well as g_1 and $\bar{R}_{ds}$, and considerably accelerate the rate of cutoff when compared with the corresponding amplifier case. Generally speaking, the conversion gain–bandwidth product increases initially as the number of sections employed is increased until the optimum number is reached. Thereafter, selective rolloff at high frequency will take place as more sections are added.

It transpires from Fig. 8 that for a given value of R_{gs}, increasing R_{OG} above 50 Ω will minimize the ill effects of gate resistive loading within the passband of the gate line. Having said that, for a given value of $\bar{C}_{gs}$, increasing R_{OG} will incur significant penalties such as reducing the bandwidth f_{CG} of the line. For example, if the line is ideal and lossless, the cutoff frequency is inversely proportional to $R_{OG}\bar{C}_{gs}$. So in cases where MESFET's with relatively large values of $\bar{C}_{gs}$ are employed, and the specified operating frequency band extends to relatively high frequency, resort

must be made to reducing R_{OG} below 50 Ω in the interest of extending the cutoff frequency and effectively reducing gate resistive loading at the high-frequency end of the specified band. The degradation of conversion gain can be compensated for by employing more sections, provided that the resultant cutoff frequency meets the specification. Whatever the case, wide-band impedance transformers are, therefore, required for matching, in addition to the m-derived matching half sections, if a line impedance of considerably higher or lower than 50 Ω is employed. Exponential tapered microstrip line [14] is an excellent choice for this purpose because it behaves approximately like a high-pass filter and its VSWR decreases rapidly with increasing frequency. Finally, to separate the IF output from the rest of the parasitic frequency components and to terminate them properly, a two-way selective wide-band filter or diplexer has been designed to terminate the m-derived matching section at the forward end of the output drain line. Emphasis is placed on achieving an input impedance that most approximates a 50-Ω pure resistance over the two frequency bands, as well as minimum interference between them. The singly loaded filter [15] proves to be especially useful here; the structure is comprised of two branches of singly loaded filters connected in parallel, namely a singly loaded Butterworth low-pass filter for retrieving the IF output signal and an identical order singly loaded Butterworth high-pass filter (that is a bandpass structure in practice) designed with the same 3-dB cutoff point to terminate some of the mixer's output parasitic frequency products. However, the output impedance of the drain line after the m-derived matching section is obviously nonzero. Nevertheless, the extra error introduced in the overall VSWR performance of the filter structure is negligible in practice. The notable feature of this arrangement is that it allows the two filters to cancel each other's susceptances over most of their own passbands, ensuring good VSWR performance.

Finally, a MESFET suitable for distributed mixer construction should meet the following criteria (in order of importance):

1) a high value of zero gate bias g_m and a steep slope in the g_m versus V_{gs} curve near gate pinchoff, to ensure maximum possible conversion transconductance and minimum LO drive requirement;
2) a low value of C_{gs} to increase signal bandwidth;
3) a low value of R_{gs} to reduce gate resistive loading;
4) a high value R_{ds} to reduce drain resistive loading;
5) low values of feedback elements like C_{dg} and R_s for reducing unwanted coupling between input gate line and output drain line.

V. Experimental Verification

To validate the concept and theory proposed, a simple two-section design has been realized in hybrid form, employing two NEC NE71000 GaAs microwave MESFET chips. The design comprises nominally 50-Ω gate and drain lines together with an external directional coupler, and was fabricated on 0.635-mm-thick and 1×1-in MRC gold-plated Alumina substrate. A photograph of the two-section design is shown in Fig. 12. Lumped components [16]–[18] are chosen because of their approximate frequency-independent properties. Gold bond wires (25 μm) were employed to simulate lumped inductors while lumped capacitors to ground were realized using low-impedance microstrip lines. Source grounding was provided by two ultrasonically drilled via-holes immediately below the MESFET chips, filled with silver-loaded conducting paint.

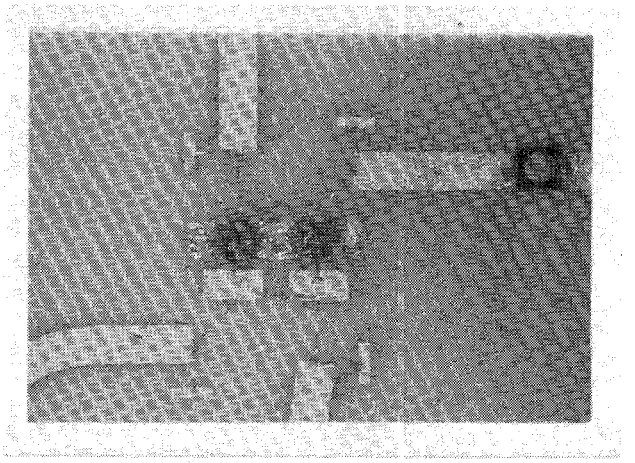

Fig. 12. A photograph of the two-section distributed mixer.

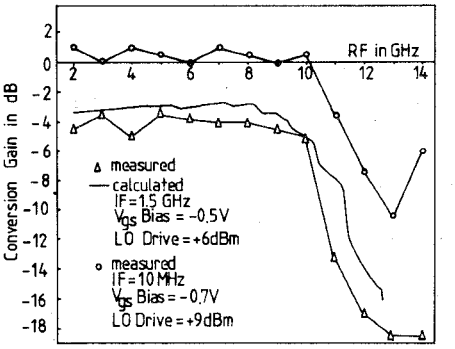

Fig. 13. Measured and calculated conversion gain versus signal RF.

The mixer conversion gain was measured using the HP(8555A/8552B) spectrum analyzer and two HP(86290B) signal generators (nonsynthesized) for providing the LO and RF signals.

The variation of measured conversion gain with signal frequency for a constant IF of 1.5 GHz is shown in Fig. 13. It demonstrates a conversion loss of 4 (+1, −0.5) dB from 2–10 GHz of RF. Good agreement with predicted results is observed, as shown in Fig. 13.

The loss reduces further to 3 (+1.5, −0.5) dB over the same frequency band under optimum gate bias and LO drive at each signal frequency. Measurements show that the conversion gain becomes positive at low IF frequency. For example, a measured conversion gain of +0.5 dB (±0.5 dB) was demonstrated for an IF of 10 MHz, as depicted in Fig. 13. The cause of this phenomenon is still under investigation.

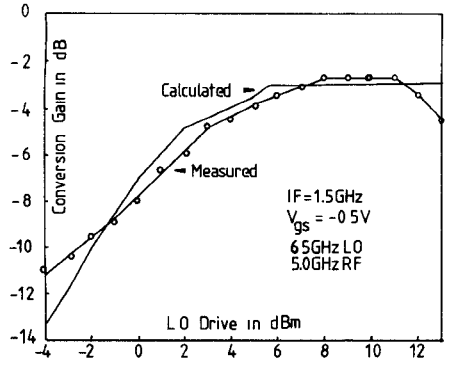

Fig. 14. Measured and calculated conversion gain versus LO drive level at 6.5-GHz LO frequency, 1.5 GHz IF and −0.5-V gate bias.

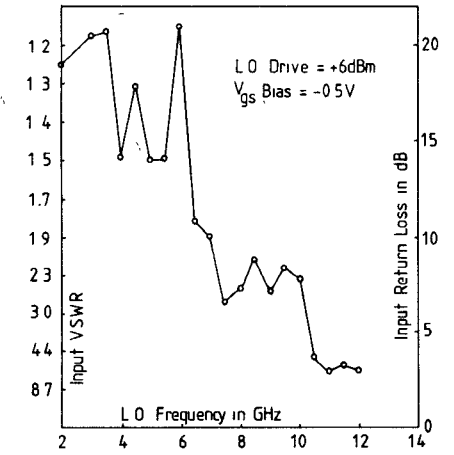

Fig. 15. VSWR and return loss of input port with external directional coupler removed versus LO frequency at 6-dBm LO drive and −0.5 V gate bias.

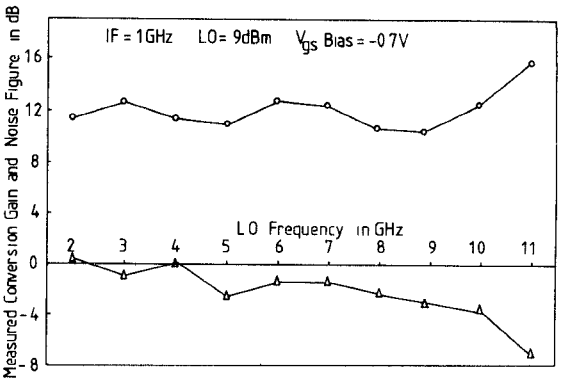

Fig. 16. Variation of noise figure and conversion gain with LO frequency at 1.0-GHz IF, 9-dBm LO drive level, and −0.7-V gate bias. ∘: Measured noise figure (single sideband). △: Measured conversion gain.

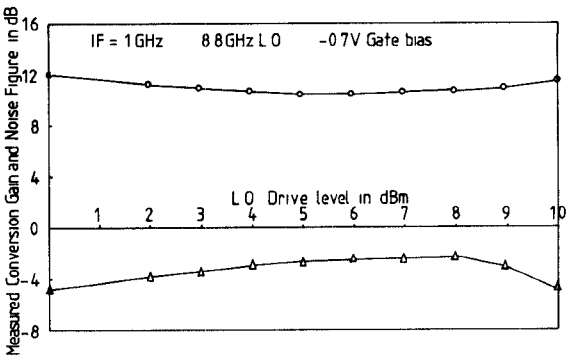

Fig. 17. Variation of noise figure and conversion gain with LO drive level at 8.8-GHz LO frequency and −0.7-V Gate Bias. ∘: Measured noise figure (single sideband). △: Measured conversion gain.

A typical variation of calculated and measured conversion gain with LO power is shown in Fig. 14. Good agreement is observed up to +11 dBm of LO power. The theory fails to predict the fall in conversion gain above +11 dBm because two effects have been neglected. Firstly, an abrupt drop in R_{ds} will result if the drain LO voltage swings beyond the current saturation region. Secondly, with even higher LO power, the gate line turns from an *LCR* transmission line to an *LR* transmission line because of the shunting effect of forward-biased leakage resistances across the gate capacitances.

The 1-dB compression point of this design occurs typically at around +5 dBm, with 11 dBm of LO drive level (at input to mixer). The IF output port exhibits an excellent return loss of greater than 23 dB up to 1.5 GHz, which is equivalent to a VSWR of lower 1.15; the return loss and VSWR of the input port with the directional coupler removed, and with +6 dBm of input power applied, are displayed in Fig. 15. The decrease in return loss above midband is due to the serious gate resistive loading of the NE71000.

Noise figure and associated conversion gain measurements were performed using the HP8970A noise figure meter and HP346B broad-band noise source. The two-section design exhibits around 10–13-dB noise figure (single sideband) for an IF band that starts from 500 MHz to 1.5 GHz. A typical set of measurements is shown in Fig. 16. Finally, Fig. 17 illustrates a typical set of measurements of noise figure and conversion gain versus LO drive level. The relatively high noise figure of this two-section design is mainly attributed to the fact that the IF signals are not selectively terminated (for example, short circuited [4]) at the two ports of the input gate line, and partly due to the fact that it is a single-ended mixer and noise from the LO can enter the system and become down converted to the IF.

We also expect the noise figure to be reduced when more sections are used (up to the optimum number), similar to the case of the distributed amplifiers [11], [19].

The objective to building this two-section distributed mixer has been fulfilled since the theory has been confirmed in practice and the conversion gain is in accordance with the theoretical predictions.

VI. Conclusion

The principle and theory of distributed (traveling-wave) mixing have been presented. A simplified unilateral nonlinear model of a GaAs MESFET has also been described. It is based on small-signal microwave *s*-parameter measurements, as well as dc and low-frequency characterizations. The impact of gate and drain loading, as well as various parasitics on circuit performance, has been assessed. In

particular, the tradeoffs between design variables to achieve a good compromise between conversion gain and RF bandwidth have been examined.

To test the validity of the theory, a two-section design has been designed and built. It exhibits around 4 dB of conversion loss over the signal-frequency band from below 2 GHz to the cutoff at 10 GHz for an IF of 1.5 GHz. Agreement with theoretical predictions is good. A noise figure of around 10 to 13 dB was also measured under the same operating conditions. Excellent IF port VSWR and good input port return loss have also been demonstrated.

Higher conversion gain–bandwidth products and lower noise figures are expected if more sections are employed and the IF signals are optimally terminated at the inputs.

ACKNOWLEDGMENT

The authors would like to thank Dr. C. Camacho-Penalosa of the Universidad Politecnica de Madrid of Spain for numerous invaluable suggestions, as well as C. L. Law of Chelsea College and A. E. Ward of Marconi for helpful discussions.

REFERENCES

[1] J. E. Sitch and P. N. Robson, "The performance of GaAs FET as microwave mixers," *IEEE Proc.*, vol. 61, pp. 399–400, Mar. 1973.
[2] R. A. Pucel, D. Masse, and R. Bera, "Performance of GaAs MESFET mixers at *X*-band," *IEEE Trans. Microwave Theory Tech.*, vol. MTT-24, pp. 351–360, June 1976.
[3] G. Begemann and A. Hecht, "The conversion gain and stability of MESFET gate mixer," in *Proc. 9th Eur. Microwave Conf.*, 1979, pp. 316–320.
[4] G. K. Tie and C. S. Aitchison, "Noise figure and associated conversion gain of a microwave MESFET gate mixer," in *Proc. 13th Eur. Microwave Conf.*, 1983, pp. 579–584.
[5] T. Hirota and H. Ogawa, "A novel *K*-band balanced FET Up-converter," *IEEE Trans. Microwave Theory Tech.*, vol. MTT-32, pp. 679–683, July 1984.
[6] O. S. A. Tang and C. S. Aitchison, "A microwave distributed MESFET mixer," in *Proc. 14th Eur. Microwave Conf.*, 1984, pp. 483–487.
[7] W. S. Percival, "Thermionic valve circuits," British Patent 460 562, 1937.
[8] Y. Ayasli, R. L. Mozzi, J. L. Vorhaus, L. D. Reynolds, and R. A. Pucel, "A monolithic GaAs 1–13 GHz traveling wave amplifier," *IEEE Trans. Microwave Theory Tech.*, vol. MTT-30, pp. 976–981, July 1982.
[9] K. B. Niclas, W. T. Wilser, T. R. Kritzer, and R. R. Pereira, "On theory and performance of solid-state microwave distributed amplifiers," *IEEE Trans. Microwave Theory Tech.*, vol. MTT-31, pp. 447–456, June, 1983.
[10] K. B. Niclas and B. A. Tucker, "On noise in distributed amplifiers at microwave frequencies," *IEEE Trans. Microwave Theory Tech.*, vol. MTT-31, pp. 661–668, Aug. 1983.
[11] C. S. Aitchison, "The intrinsic noise figure of the MESFET distributed amplifier," *IEEE Trans. Microwave Theory Tech.*, vol. MTT-33, pp. 460–466, June 1985.
[12] E. O. Brigham, *The Fast Fourier Transform*. Englewood Cliffs, NJ: Prentice-Hall, 1974.
[13] C. Camacho-Penalosa and C. S. Aitchison, "Modelling frequency dependence of output impedance of a microwave MESFET at low frequencies," *Electron. Lett.*, vol. 21, no. 12, pp. 528–529, June 1985.
[14] P. Pramanick and P. Bhartia, "Tapered microstrip transmission lines," in *IEEE Int. Microwave Symp. MTT-S Dig.*, 1983, pp. 242–244.
[15] G. L. Matthaei, L. Young, and E. M. T. Jones, *Microwave Filters, Impedance-Matching Networks, and Coupling Structures*. New York: McGraw-Hill, 1964.
[16] C. S. Aitchison *et al.*, "Lumped-circuit elements at microwave frequencies," *IEEE Trans. Microwave Theory Tech.*, vol. MTT-19, pp. 928–937, Dec. 1971.
[17] R. S. Pengelly and D. C. Rickard, "Design, measurement and application of lumped elements up to *J*-band," in *Proc. 7th Eur. Microwave Conf.*, 1977, pp. 460–463.
[18] J. B. Klatskin and R. L. Camisa, "Fabrication of lumped element broadband GaAs MESFET microwave power amplifiers," *RCA Rev.*, vol. 42, pp. 576–595, Dec. 1981.
[19] N. Nazoa-Ruiz and C. S. Aitchison, "Experimental gain and noise figure performance of distributed MESFET amplifiers," *Electron. Lett.*, vol. 21, no. 5, pp. 196–197, Feb. 1985.

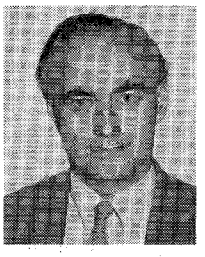

Colin S. Aitchison was born in Morecambe, England, in 1933. He received the B.Sc. and A.R.C.S. degrees in physics from Imperial College, London University, London, England, in 1955.

He worked for Philips Research Laboratories, Redhill, Surrey, England, from 1955 to 1972, being initially concerned with the noise-reduction properties of direct injection phase-locked klystrons for use with Doppler radars. He led a group concerned with parametric amplifiers, mixers, ferrite limiters, lumped microwave components, and Gunn and Avalanche oscillators.

In 1972, he joined the Department of Electronics, Chelsea College, University of London, London, England, where he was Professor in Electronics. He has recently joined ERA Technology Ltd at Leatherhead, Surrey, England. His research interests remain in the field of active microwave circuits, particularly distributed amplifiers.

Prof. Aitchison is a Fellow of the Institution of Electrical Engineers, a Member of the Institute of Physics, and an Emeritus Professor of the University of London.

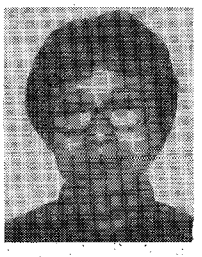

On San Andy Tang was born in Hong Kong in 1959. He received the B.Sc.(Eng.) degree with first class honors in electronic engineering from Chelsea College (now renamed King's College (KQC)), University of London, England, in 1982. He then joined the Microwave Research Group of the same department, where he was supported by Marconi Defence Systems, Ltd., Stanmore, England, to work towards a Ph.D. degree in the area of MESFET mixers and wide-band microwave circuits.

Since November 1985, he has been with the Microwave Group of the Advanced Technology Department of Marconi in Stanmore, where he is engaged in R&D on multioctave microwave linear and nonlinear circuits and devices, and especially distributed mixers and amplifiers. Since 1982, he has been a holder of the O.R.S. Awards of U.K. C.V.C.P. and has been an associate member of the IEE.